

IL NUOVO CIMENTO **39 C** (2016) 372

DOI 10.1393/ncc/i2016-16372-0

COLLOQUIA: SEA2016

## Cluster structure of neutron-rich $^{10}\text{Be}$ and $^{14}\text{C}$ via resonant alpha scattering

D. SUZUKI<sup>(1)</sup>, T. AHN<sup>(2)</sup>, D. BAZIN<sup>(3)</sup>, F. D. BECCHETTI<sup>(4)</sup>, S. BECEIRO-NOVO<sup>(3)</sup>,  
A. FRITSCH<sup>(5)</sup>, J. J. KOLATA<sup>(2)</sup> and W. MITTIG<sup>(3)</sup> for the AT-TPC COLLABORATION

<sup>(1)</sup> *RIKEN Nishina Center - Wako, Saitama, Japan*

<sup>(2)</sup> *Department of Physics, University of Notre Dame - Notre Dame, IN, USA*

<sup>(3)</sup> *National Superconducting Cyclotron Laboratory, Michigan State University  
East Lansing, MI, USA*

<sup>(4)</sup> *Department of Physics, Randall Laboratory, University of Michigan  
Ann Arbor, MI, USA*

<sup>(5)</sup> *Gonzaga University, Department of Physics - Spokane, WA, USA*

received 28 November 2016

**Summary.** — Neutron-rich  $^{10}\text{Be}$  and  $^{14}\text{C}$  nuclei were studied via resonant  $\alpha$  scattering of radioactive  $^6\text{He}$  and  $^{10}\text{Be}$  beams, respectively, produced by the *TwinSol* facility at the University of Notre Dame. The Prototype Active-Target Time-Projection Chamber (pAT-TPC) was used as a thick gaseous  $\alpha$  target to induce resonant scattering and as a device to track reacted particles inside the target, providing continuous excitation functions and angular distributions over a wide range of energies and angles. The experimental results indicate a melting phenomenon of  $\alpha$  clusters in the  $4^+$  rotational member of the  $^{10}\text{Be}$  ground state and a linear chain alignment of three  $\alpha$  clusters in  $^{14}\text{C}$  excited states, as recently predicted by an anti-symmetrized molecular dynamics calculation.

### 1. – Introduction

Studies of  $\alpha$  clustering, dated back to as far as the 1930s [1], still constitute the forefront in modern nuclear physics. Neutron-rich nuclei have increasingly attracted attention in recent years. If clustering occurs, these nuclei represent a hybrid system, where excess neutrons around  $\alpha$  clusters add another degree of freedom, prompting questions on whether  $\alpha$  clusters in stable nuclei with equal numbers of protons ( $Z$ ) and neutrons ( $N$ ) persist as they are, or change their cluster properties such as geometrical alignment, or even dissolve into a shell-model-like state. Neutron-rich  $^{10}\text{Be}$  and  $^{14}\text{C}$  are very important nuclei to answer these questions since their  $N = Z$  isotopes,  $^8\text{Be}$  and  $^{12}\text{C}$ , have arguably the best established cluster states, that are even reproduced by *ab initio* calculations using bare nuclear forces [2, 3]. Previous theoretical studies by the molecular

orbital model [4], the anti-symmetrized molecular dynamics (AMD) approach [5-7], the multicluster generator coordinate method [8], and full [9,10] or semi microscopic cluster models [11] show that the two valence neutrons of  $^{10}\text{Be}$  and  $^{14}\text{C}$  significantly impact the  $\alpha$  clustering, predicting molecular neutron orbitals [4], or linear chain alignment of  $\alpha$  clusters [7], the phenomenon that was first conjectured for the  $N = Z$  nuclei [12], but remains unidentified even for the simplest  $3\alpha$  case in  $^{12}\text{C}$  [13,14]. While a number of experiments have been carried out [15-22], most of the predicted cluster states remain unknown or to be studied.

We studied  $^{10}\text{Be}$  [23] and  $^{14}\text{C}$  [24] via  $\alpha$  resonant scattering off radioactive  $^6\text{He}$  and  $^{10}\text{Be}$  beams, respectively. The active target and time-projection chamber, Prototype AT-TPC (pAT-TPC) [25] containing He and  $\text{CO}_2$  gas mixture was used as a reaction target as well as tracking medium of charged particles. The thick target method [26], where excitation functions are measured by decelerating beam particles over the length of a thick target, was used. Measuring reaction trajectories inside the target, commonly called active target technique [27], allows one to directly determine the reaction vertex and unambiguously deduce the beam energy, which translates into the resonance energy [23,24,28]. This would otherwise be limited with the widely-used multiple silicon detector setup that indirectly determines the reaction vertex, by assuming reaction kinematics energetically allowed, from the energy and angle of an  $\alpha$  particle after leaving the target. The active target method enables the measurement of wide-ranging and continuous excitation functions and angular distributions, facilitating the identification of unknown resonances and oscillatory diffraction patterns, which are the most reliable information in determining the spin and parity.

## 2. – Experiment

These measurements were performed as the first series of experiments of the pAT-TPC using *TwinSol* [29] radioactive-ion beams at the FN tandem accelerator facility of the University of Notre Dame [30].  $^6\text{He}$  ions were produced via the ( $d, ^3\text{He}$ ) reaction using a deuterium target at 1200 mm-Hg and 29.2 MeV  $^7\text{Li}$  (3+) primary beam. To produce  $^{10}\text{Be}$  ions, a stack of four 0.1 mg/cm<sup>2</sup> thick  $^{13}\text{C}$  targets were bombarded by a 46 MeV  $^{11}\text{B}$ (5+) primary beam. Radioactive ions thus produced were collected and purified in flight by the *TwinSol* device [29] consisting of a pair of solenoidal magnets. The secondary beam was delivered to the cylindrical target volume of He:CO<sub>2</sub> 90:10 mixture gas at 1 atm of the pAT-TPC [25], measuring 50 cm along the beam axis and 27 cm in diameter. The beam energies of  $^6\text{He}$  and  $^{10}\text{Be}$  were 15 and 40 MeV, respectively. The corresponding center-of-mass energies  $E_{c.m.}$  (6 MeV for  $^6\text{He}$  and 11.3 MeV for  $^{10}\text{Be}$ ) decreased to zero while travelling the length of the gas volume. The average rate of  $^6\text{He}$  that entered the volume was  $2 \times 10^3$  ions per second with a purity of 90%. The main impurity was  $^4\text{He}$ . The average rate of  $^{10}\text{Be}$  was  $10^3$  ions per second. The beam purity was about 35% with main contaminants of  $^4\text{He}(2+)$  (50%),  $^9\text{Be}(4+)$  (5%), and  $^{10}\text{B}(4+)$  (3%). Electrons from reaction trajectories are guided toward the Micromegas amplifier [31] by an electric field of 0.8 kV/cm parallel to the beam axis. The Micromegas consists of 2 mm wide radial strips separated into quadrants. A waveform digitizer [32] records the charge as a function of drift time over 40  $\mu\text{s}$  by using an array of 511 switching capacitors.

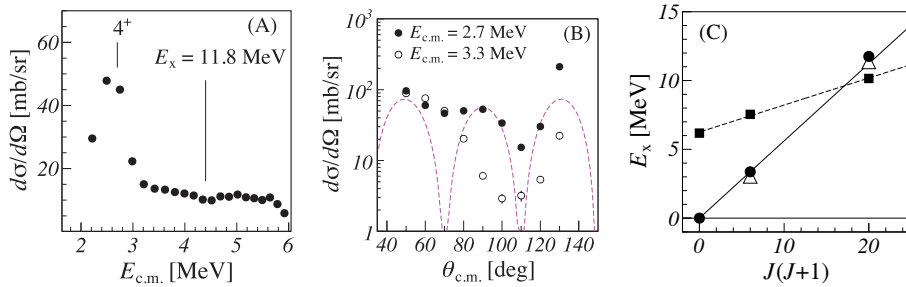


Fig. 1. – (A) Excitation function for  $^6\text{He} + \alpha$  elastic scattering. The data are integrated over  $\theta_{c.m.} = 65^\circ\text{--}135^\circ$ . The observed  $4^+$  resonance at around  $E_{c.m.} = 2.7$  MeV and the missing  $4^+$  resonance expected from a  $^{10}\text{Be}$  state at  $E_x = 11.8$  MeV are denoted by the lines. (B) Differential cross sections of  $^6\text{He} + \alpha$  elastic scattering for the  $4^+$  resonance at  $E_{c.m.} = 2.7$  MeV (filled circles). Off-resonance data at 3.3 MeV (open circles) are also shown for reference. The oscillatory pattern of the 2.7 MeV data agrees with that of the squared Legendre function with  $L = 4$  (dashed line), for which an arbitrary scaling factor was adopted for presentation purposes. (C) Excitation energies *vs.*  $J(J + 1)$  plot for rotational band members of the ground (circles) and second (squares)  $0^+$  states of  $^{10}\text{Be}$ . The ground-state band members of  $^8\text{Be}$  (triangles) are also shown for comparison.

### 3. – Results

The angle-integrated excitation function for  $^6\text{He}$  elastic scattering is shown in fig. 1(A). While elastic scattering was previously measured at several beam energies [15-17,19], this is the first differential cross section data taken continuously over a finite range of energy. The resonance visible at  $E_{c.m.} = 2.56(15)$  MeV is assigned a spin and parity of  $4^+$  from the diffraction seen in the angular distribution of fig. 1(B), which excellently agrees with the oscillatory pattern of the squared Legendre function for an angular momentum  $L = 4$ . The partial  $\alpha$  decay width was estimated to be  $\Gamma_\alpha/\Gamma = 0.49(5)$  from the resonance cross sections. These results are in line with the previous measurement with a narrower energy range, but with better statistics [19]. The large partial width of this  $4^+$  state, widely considered as the  $4^+$  member of the second  $0^+$  rotational band, supports the predicted  $\sigma$ -type molecular orbital structure around the two  $\alpha$  clusters [4,5]. Another  $4^+$  state of the ground state  $0^+$  band, often discussed as a  $\pi$ -type partner of the second  $0^+$  band, is predicted at  $E_{c.m.} = 3$  to 6 MeV by several calculations [4-6, 8, 10, 11]. This state has been associated with a  $^{10}\text{Be}$  level found at an excitation energy ( $E_x$ ) of 11.76 MeV [20], or  $E_{c.m.} = 4.36$  MeV, given the  $\alpha$  emission threshold at  $E_x = 7.4$  MeV. However, our result that allowed us to survey a wide range of excitation energies up to  $E_{c.m.} = 6$  MeV rules out resonances at predicted energies, with an upper limit of  $\Gamma_\alpha = 20$  keV. This is almost one order of magnitude small than that of the 2.56 MeV resonance with  $\Gamma_\alpha = 145(15)$  keV. The missing resonance strength and the hindered branching for  $\alpha$  emission indicate that the degree of clusterization is reduced in the  $4^+$  state of the ground state  $0^+$  rotational band. The weakening of clustering is pointed out by an early AMD study of  $^{10}\text{Be}$  [5], predicting that the  $\alpha$  clusters in the  $0^+$  ground state gradually dissolve in the rotational band members as the total spin increases. It is interesting to note that the ground state band of  $^{10}\text{Be}$  has almost the same level spacing as  $^8\text{Be}$  (fig. 1(C)), while the  $\alpha$  clustering in  $^8\text{Be}$  appears to be robust in  $0^+$ ,  $2^+$ , and  $4^+$  states. The  $\alpha$  spectroscopic factors of  $^8\text{Be}$  are equally large in all of

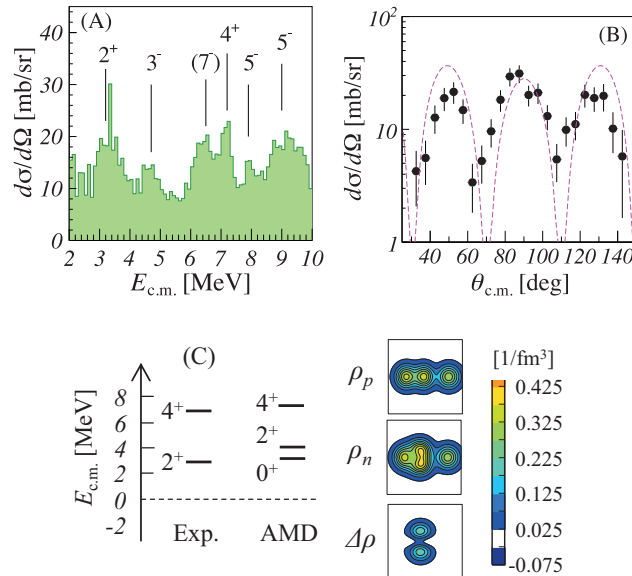


Fig. 2. – (A) Excitation function for  $^{10}\text{Be} + \alpha$  elastic scattering. Resonances of  $^{14}\text{C}$  and their spins and parities from the present analysis are shown. (B) Differential cross sections of  $^{10}\text{Be} + \alpha$  elastic scattering for the resonance at  $E_{c.m.} = 7.0$  MeV (filled circles). The oscillatory pattern agrees with that of the squared Legendre function with  $L = 4$  (dashed line), for which an arbitrary scaling factor was used. (C) Comparison of the  $2^+$  and  $4^+$  resonance energies to the linear  $3\alpha$  chain states predicted in a  $\beta$ - $\gamma$  constraint AMD study [7]. The proton ( $\rho_p$ ) and neutron ( $\rho_n$ ) density distributions and their differential ( $\Delta\rho = \rho_p - \rho_n$ ) for the predicted linear chain states are displayed.

these states according to the folding-model potential calculation that well describes the level energies and widths of these states [33]. In one *ab initio* Quantum Monte Carlo calculation of  $^8\text{Be}$  [2], the density distribution of the  $4^+$  state shows the two  $\alpha$  clusters as clearly as in the  $0^+$  ground state. The dissociation of  $\alpha$  clusters in  $^{10}\text{Be}$ , which thus stands in stark contrast with  $^8\text{Be}$ , may be due to the two excess neutrons that complete the filling of the  $1p_{3/2}$  orbital. The large energy gap relative to the higher  $1p_{1/2}$  orbital that gives rise to the subshell closure at  $N = 6$  may favour shell-model-like structure over the  $\alpha$  clustering.

The excitation function for elastic  $\alpha$  scattering of  $^{10}\text{Be}$  is shown in fig. 2(A). Among several resonances of  $^{14}\text{C}$  identified, there are two positive-parity states, one being a  $2^+$  state at  $E_{c.m.} = 3.0$  MeV, the other a  $4^+$  state at 7.0 MeV. These spin and parity assignments were made again from the oscillation patterns of differential cross sections (fig. 2(B)). These levels are compared to a  $\beta$ - $\gamma$  constraint AMD calculation using the generator coordinator method [7] in fig. 2(C). The experimental resonance energies well agree with the  $2^+$  and  $4^+$  states of one of the rotational bands predicted. As seen in the intrinsic density distributions, three  $\alpha$  clusters are aligned in a linear arrangement in this band. This supports the presence of a linear  $3\alpha$  chain structure in excited states of  $^{14}\text{C}$ .

#### 4. – Summary

To study the cluster structure of  $^{10}\text{Be}$  and  $^{14}\text{C}$ , resonant  $\alpha$  scattering of radioactive  $^6\text{He}$  and  $^{10}\text{Be}$  beams was measured at the *TwinSol* facility using the pAT-TPC. The hindered branching for  $\alpha$  emission observed for the  $4^+$  rotational member of the  $^{10}\text{Be}$  ground state indicates that the  $\alpha$  clustering of the ground state, consistently predicted by different theoretical studies, fades away in the  $4^+$  rotational member. The newly-found  $2^+$  and  $4^+$  states of  $^{14}\text{C}$  agree with linear chain states predicted by the recent AMD work. The  $\alpha$  clustering is robust against dissociation in  $^8\text{Be}$  and the linear chain structure is predicted to be manifested very weakly in  $^{12}\text{C}$ . The present results suggesting these phenomena realized in  $^{10}\text{Be}$  and  $^{14}\text{C}$  indicate that two valence neutrons alone can drastically and essentially evolve the  $\alpha$  cluster structure.

\* \* \*

This work was supported by the National Science Foundation under Grant Nos. PHY09-69456, PHY14-01343, PHY14-19765, PHY14-30152, and MRI09-23087.

#### REFERENCES

- [1] WHEELER J. A., *Phys. Rev.*, **52** (1937) 1083.
- [2] WIRINGA R. B., *Phys. Rev. C*, **62** (2000) 014001.
- [3] EPELBAUM E. *et al.*, *Phys. Rev. Lett.*, **109** (2012) 252501.
- [4] ITAGAKI N. and OKABE S., *Phys. Rev. C*, **61** (2000) 044306.
- [5] KANADA-EN'YO Y. *et al.*, *Phys. Rev. C*, **60** (1999) 064304.
- [6] SUHARA T. and KANADA-EN'YO Y., *Prog. Theor. Phys.*, **123** (2010) 303.
- [7] SUHARA T. and KANADA-EN'YO Y., *Phys. Rev. C*, **82** (2010) 044301.
- [8] DESCOUVEMONT P., *Nucl. Phys. A*, **699** (2002) 463.
- [9] ITO M. *et al.*, *Phys. Lett. B*, **588** (2004) 43.
- [10] HERNÁNDEZ DE LA PEÑA L. *et al.*, *J. Phys. G*, **27** (2001) 2019.
- [11] ARAI K., *Phys. Rev. C*, **69** (2004) 014309.
- [12] MORINAGA H., *Phys. Rev.*, **101** (1956) 254.
- [13] NEFF T. and FELDMEIER H., *Nucl. Phys. A*, **738** (2004) 357.
- [14] SUHARA T. and KANADA-EN'YO Y., *Prog. Theor. Phys.*, **123** (2010) 303.
- [15] TER-AKOPIAN G. M. *et al.*, *Phys. Lett. B*, **426** (1998) 251.
- [16] RAABE R. *et al.*, *Phys. Lett. B*, **458** (1999) 1.
- [17] RAABE R. *et al.*, *Phys. Rev. C*, **67** (2003) 044602.
- [18] VON OERTZEN W. *et al.*, *Eur. Phys. J. A*, **21** (2004) 193.
- [19] FREER M. *et al.*, *Phys. Rev. Lett.*, **96** (2006) 042501.
- [20] BOHLEN H. G. *et al.*, *Phys. Rev. C*, **75** (2007) 054604.
- [21] HAIGH P. J. *et al.*, *Phys. Rev. C*, **78** (2008) 014319.
- [22] FREER M. *et al.*, *Phys. Rev. C*, **90** (2014) 054324.
- [23] SUZUKI D. *et al.*, *Phys. Rev. C*, **87** (2013) 054301.
- [24] FRITSCH A. *et al.*, *Phys. Rev. C*, **93** (2016) 014321.
- [25] SUZUKI D. *et al.*, *Nucl. Instrum. Methods Phys. Res. A*, **691** (2012) 39.
- [26] ARTEMOV K. P. *et al.*, *Sov. J. Nucl. Phys.*, **55** (1992) 1460.
- [27] BECEIRO-NOVO S. *et al.*, *Prog. Part. Nucl. Phys.*, **84** (2015) 124.
- [28] SAMBI S. *et al.*, *Eur. Phys. J. A*, **51** (2015) 25.
- [29] BECCHETTI F. *et al.*, *Nucl. Instrum. Methods Phys. Res. A*, **505** (2003) 377.
- [30] AHN T. *et al.*, *Nucl. Instrum. Methods Phys. Res. B*, **376** (2016) 321.
- [31] GIOMATARIS Y. *et al.*, *Nucl. Instrum. Methods Phys. Res. A*, **376** (1996) 29.
- [32] BARON P. *et al.*, *IEEE Trans. Nucl. Sci.*, **NS-55** (2008) 1744.
- [33] MOHR P. *et al.*, *Z. Phys. A*, **349** (1994) 339.